IAWA Journal, Vol. 27 (1), 2006: 3–17

MAGNETIC RESONANCE MICRO-IMAGING OF XYLEM SAP DISTRIBUTION AND NECROTIC LESIONS IN TREE STEMS

Keiko Kuroda[1], **Yoshiyuki Kanbara**[2], **Takashi Inoue**[3] and **Akira Ogawa**[3]

SUMMARY

To get high quality magnetic resonance (MR) micro-images for the physiological and anatomical investigation of tree stems, the imaging with various combinations of parameters was tested on a Signa VH/i 3.0 T MR imaging system (General Electric Medical Systems). Proton density and T2 weighted spin echo (SE) sequences are commonly used to detect areas with abundant water. Cambial zone and the area consisting of water-filled conduits looked whitish in the MR images of healthy *Pinus densiflora* and *Quercus serrata* stems that were obtained by these sequences. In the MR images of diseased *P. densiflora* that had been inoculated with a wilt pathogen, *Bursaphelenchus xylophilus*, the area dehydrated as a result of embolism appeared pitch-black. In the images of diseased *Quercus crispula* saplings, that had been inoculated with the wilt pathogen *Raffaelea quercivora*, the dehydrated xylem was shown as a dark area. The T1 weighted SE or gradient echo (FSPGR) sequence, that is used to detect fat and protein distribution, provided high intensity MR signals for the pathogenic heartwood and necrotic areas resulting from fungal activity. The resolution of MR images obtained by SE sequences was estimated 100–150 μm from the FOV and image size. The data sets obtained by the FSPGR sequence that consist of 0.8 mm thick serial sections enables the three-dimensional analysis of the affected area. This technique is helpful for detecting the water distribution and areas affected by pathogenic microorganisms in living tree stems.

Key words: MRI, NMR, ater conductivity, infection, T1, nondestructive.

INTRODUCTION

It is well known that the physiological conditions of trees fluctuate depending on the water status of their trunks (Kozlowski & Pallardy 1997). The hydraulic conductivity of the xylem is a very important factor in tree health. Water-stressed trees tend to

1) Kansai Research Center, Forestry and Forest Products Research Institute, Momoyama, Fushimi, Kyoto 612-0855, Japan [E-mail: keiko@affrc.go.jp].
2) High Field Magnetic Resonance Imaging Research Institute, Iwate Medical University, Takizawa-Mura, Iwate 020-0173, Japan.
3) Department of Neurosurgery, Iwate Medical University School of Medicine, Morioka 020-8505, Japan.

Associate Editor: John Sperry

become infected with diseases and suffer from the development of subsequent symptoms (Manion & Griffin 1992; Kuroda 2002, 2003). On the other hand, the mortality of trees infected with wilt diseases, such as pine wilt, Guignardia dieback, or an oak vascular disease caused by *Raffaelea quercivora* Kubono *et* Shin. Ito, is determined by the extent of xylem dysfunction (Kuroda 1991, 2003; Kuroda &Yamada 1996). The assessment of tree vitality in relation to xylem water conduction, however, has been difficult in living materials due to the requirement of destructive measurements. For instance, the dye injection method, which is conveniently applied to trace the sap ascent in tree stems (Kuroda *et al*. 1988; Sakamoto *et al*. 2004), requires that trees be cut, making repeated analysis on the same tree impossible.

In tree physiology, anatomy, and pathology, there is a strong interest in achieving noninvasive investigations on living trees. The acoustic emission technique (Tyree & Sperry 1989; Kuroda 2002), the impulse radar-wave system (microwave) (Yamaguchi *et al*. 2003), or X-ray CT (Fromm *et al*. 2001), have been used to check water conduction or distribution in trees; however, they do not provide detailed enough information on the hydraulic function of sapwood. As a noninvasive technique, magnetic resonance imaging (MRI or NMR), which was developed for medical purposes to detect lesions in human organs, is increasingly used on plants. This technique uses the behavior of protons under the magnetic field and, therefore, the distribution of water, which contains hydrogen, is detectable in the tissue. In addition to the water distribution, anomalies in diseased tissue are detectable by a kind of signal enhancement such as T1 weighting (NessAiver 1996; Bucur 2003). In recent years, MR imaging has been applied to detect water distribution in seeds, primary tissues of herbaceous plants (Glidewell *et al*. 1999; Robinson *et al*. 2000; Pietrzak *et al*. 2002), and vines (Schneider *et al*. 2000; Holbrook *et al*. 2001). Barry *et al*. (2001) and Pearce *et al*. (1997) showed that xylem with higher moisture contents formed by infection was detectable by MR imaging. In those reports, however, the resolution of the MR images is too low to analyse the conductivity of water conduits in woody stems. Detectable incidences by MR imaging and the image qualities are known to vary with the combination of parameters during scanning such as repetition time (TR), echo time (TE), field of view (FOV) and several other factors (Elster 1994). Quality of images also varies depending on the slice thickness and spacing. Improvement of the imaging sequence and parameters to obtain images suitable for physiological and pathological studies of trees is clearly needed. The present report focuses on refining the technique to get images of water-filled and dehydrated areas in healthy trees, and of the areas affected by infection in diseased trees. Such images, obtained non-destructively, will provide information to fill the gap between tree physiology and functional anatomy and help the development of tree pathology.

MATERIALS AND METHODS

Plant materials

Healthy trees in which xylem is normally conducting were analyzed first. As representative softwood and hardwood trees, *Pinus densiflora* Sieb. *et* Zucc. and *Quercus serrata* Thunb., both about 3–4 cm in stem or branch diameter, were selected (Table 1, Fig. 1). *Quercus serrata* is a ring-porous, deciduous oak (Fig. 1d). Material was

Table 1. Specimens used for MR imaging.

Condition	Species	Age (year)	Diameter (cm)	Treatment/Pathogen (disease)	Images
Healthy	*Pinus densiflora*	4	4	None	Fig. 1a, 1c, 2
	Quercus serrata	3	3	None	Fig. 1b, 1d, 3
Infected	*Pinus densiflora*	2	1	*Bursaphelenchus xylophilus* (Pine wilt)	Fig. 4
	Quercus crispula (Tree A & B)	5	4	*Raffaelea quercivora* (wilt disease)	Fig. 5, 6
Control	*Quercus crispula*	5	4	Wound	

Abbreviations in Figures 1–6: AP: axial parenchyma – Cor: cortex – CW: compression wood – CX: conducting xylem – Cz: cambial zone – Dis: discolored xylem – DX: dehydrated xylem – Ino: inoculated site – LV: large vessel – LW: latewood – P: pith – R: ray tissue – RC: resin canal – SV: small vessel.

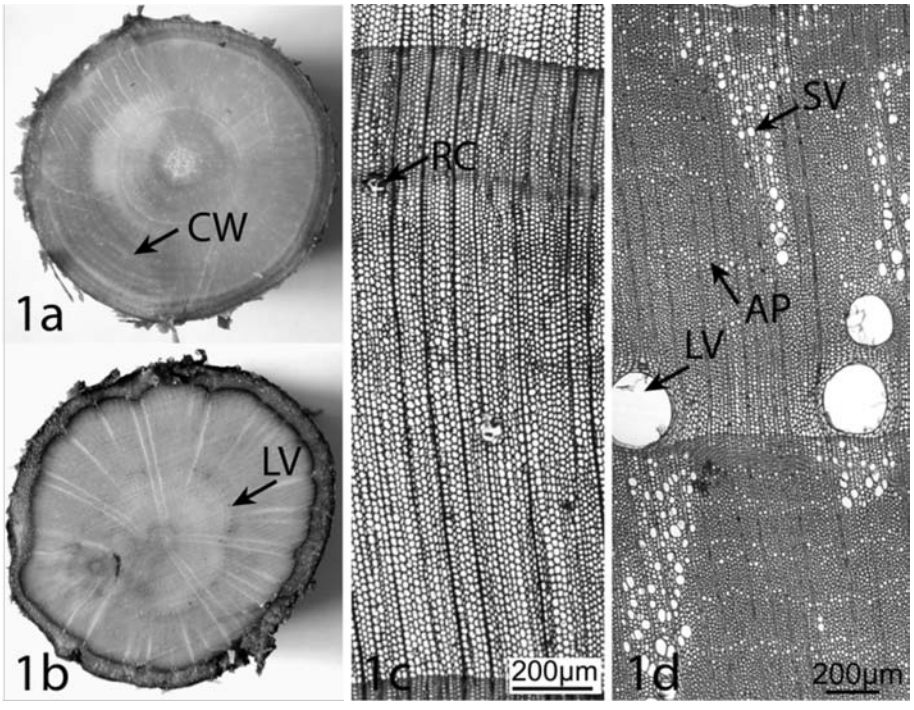

Fig. 1. Optical crosscut images of healthy trees and microscopic images of their xylem. – a & c: *Pinus densiflora* stem. – b & d: *Quercus serrata* branch.

destructively harvested in this experiment prioritizing the convenient observation prior to the non-destructive experiments. The main stem of a *P. densiflora* sapling and a long branch of *Q. serrata* that were vigorously growing in the nursery of the Kansai Research Center, Forestry and Forest Product Research Institute, Kyoto, Japan were cut at the base on September 25, 2001.

Trees inoculated with pathogens but not wilting were selected (Table 1) in order to get clear images of partially dehydrated xylem, and to detect other changes caused by infection such as necrosis. As a softwood species, a 2-year-old *Pinus densiflora* seedling that had been inoculated with the pathogenic nematode of pine wilt, *Bursaphelenchus xylophilus* (Steiner *et* Buhrer) Nickle, on July 2000 on the lower stem, was uprooted at the nursery on September 25, 2001. In pine trees infected with pine wilt, dehydration and desiccation in sapwood has earlier been shown to be associated with unrecoverable cavitation (embolism) of tracheids (Kuroda *et al.* 1988; Kuroda 1991).

Two 5-year-old saplings of *Quercus crispula* Blume (Tree A and B) that had been inoculated with the pathogenic fungus of a wilt disease, *Raffaelea quercivora*, on July 2001 were cut at the base on November 5, 2001. Inoculation in the oak trees had been made on the lower stem with additional wounds above and below the inoculation site to promote infection. As a control, a *Q. crispula* sapling inoculated with an agar medium without the pathogen was harvested. Like *Q. serrata, Q. crispula* is also a deciduous, ring-porous species.

Before the imaging, a whole *Pinus densiflora* seedling about 1 cm in stem diameter and 30 cm in height was covered with a plastic bag. The rest of the long specimens were cut into bolts of 60 cm long. Vaseline was applied on the cut ends immediately, and each bolt was wrapped with plastic films to avoid desiccation. Three cut bolts from each specimen were set together in the MR imaging system. MR images were obtained at the middle of those bolts where the effect of embolism at harvesting must have been minimal.

Magnetic resonance imaging and anatomy

MR images were obtained from a Signa VH/i 3.0 T MR imaging system (General Electric Medical Systems, Milwaukee, WI, U.S.A.) installed in the High Field Magnetic Resonance Imaging Research Institute at Iwate Medical University. The magnetic field strength was 3.0 Tesla. The bore diameter was 55 cm and the coil diameter was 7 cm. MR imaging is categorized into two by the type of MR signals as cited in Table 2: a two-dimensional spin echo (SE and FSE) and three-dimensional spoiled gradient recalled acquisition in steady-state sequences (FSPGR). Three types of signal-weighted sequences, proton density, T1, and T2 weighted sequences, were used for the different observations described below. These sequences are determined by the combination of parameters such as repetition time (TR) and echo time (TE) (NessAiver 1996). Usually, proton density weighted SE sequence is used to demonstrate water distribution. T1 weighted sequence is used to detect protein and fat, and T2 weighted sequence is used to detect water or blood in medical analysis. Combinations of the TR, TE, flip angle (FA), and slice thickness were modified to produce the best images (Table 2).

Table 2. Representative parameters used for MR imaging of woody plants.

Dimension	Sequence		Weighted sequence	TR (msec)	TE (msec)	FA deg.	NEX	Slice thickness (mm)
2D	Spin echo	SE	Proton density weighted	2000	12	90	1	3.0–5.0
		SE		4000	21	90	4	3.0–5.0
		FSE		2000	20–25	90	1	3.0–3.5
		SE	T1 weighted	540	20	90	6	3.0
		SE		800	11	90	1	3.0
		SE		1000	22	90	2	4.0
		FSE	T2 weighted	4000	80	90	4	3.0
3D	Gradient echo	FSPGR	T1 weighted	8.3	2	15	8	0.8

To obtain good contrast images of water distribution in the tree tissue, proton density SE and FSE (fast spin echo) sequences was applied. TR and TE were first adjusted to around 2000 ms and 12 ms, respectively, and then FSE sequence with longer TE was tested. T2 weighted images that also demonstrate water distribution were acquired by the FSE sequence with long TR of 4000 ms and shorter TE of 80 ms, and were compared with proton density weighted images. To get images that provide information on the effects of infection, T1 weighted sequence was tested by the combination of TR shorter than 800 ms and TE shorter than 20 ms with some modification. T1 weighted images were also obtained by 3D-FSPGR sequences, with TR, 8.3 ms and TE, 2.0 ms and with some modification (Table 2). A field of view (FOV) of 60, 80, 200 or 240 mm was used. The image size was 512 × 512 pixel. Slice thickness varied from 0.8 to 5.0 mm. The MR datasets were analyzed using the software ExsaVision Lite (Ziosoft Inc., Japan). Three-dimensional analysis was made with the data obtained by 3D-FSPGR sequences that consists of 120 to 200 sequential sections of 0.8 mm thick. Surface rendering of the 3-D datasets was carried out using the software OsiriX Ver. 1.6 (Rosset *et al*. 2004).

Just before the MR imaging, normally conducting xylem area was distinguished from the dry zone (Hillis 1987) on the cut ends of healthy specimens with the naked eye. Or after the imaging, dehydrated xylem area shown as white patches on the stem cross sections, necrosis of cambial region, and xylem discoloration were observed by dissecting specimens under a stereomicroscope (cf. Kuroda *et al*. 1988; Kuroda 1991; Kuroda &Yamada 1996). Some of the specimens were sectioned with a sliding microtome and processed for microscopy.

RESULTS

MR imaging of healthy pine and oak trees

The major part of the xylem of a healthy *Pinus densiflora* stem was judged to be conductive and filled with water by optical observations of the crosscut surface at harvest (Fig. 1a) and based on our results from previous studies of xylem dysfunction

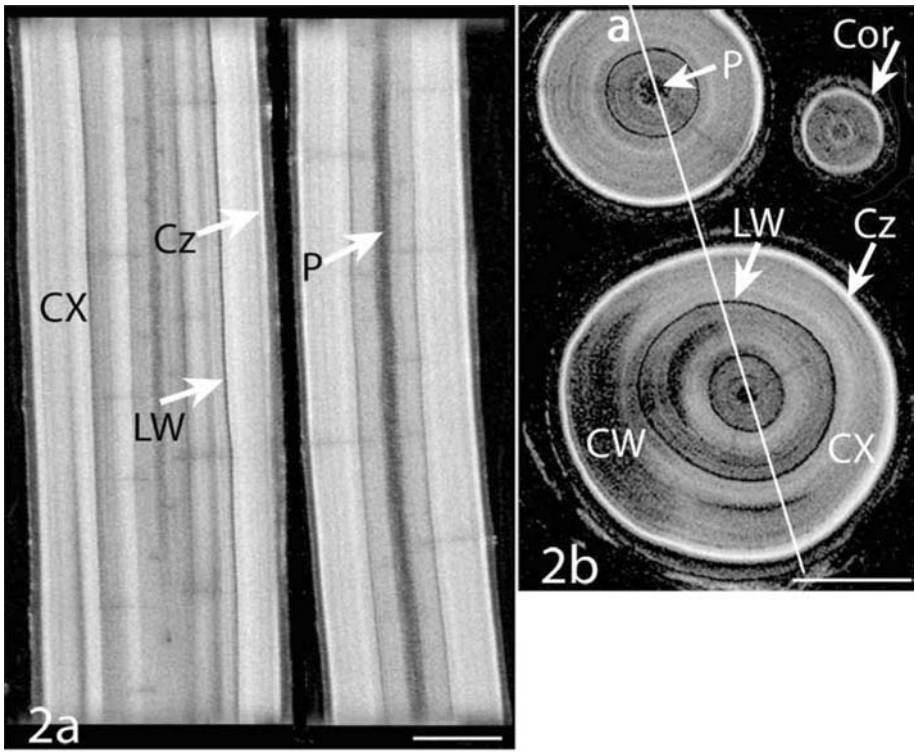

Fig. 2. Two-dimensional MR images of a healthy *Pinus densiflora* stem obtained by a spin echo (SE) sequence. – a: Proton density radial images obtained from a section cut at the solid line 'a' in Fig. 2b. TR, 2000 ms; TE, 12 ms. Pixel size 156 μm. – b: T2 weighted crosscut images. TR, 4000 ms; TE, 80 ms. Pixel size 117 μm. — Scale bar = 1 cm.

(Kuroda *et al*. 1988; Kuroda 1991). Figure 2a shows the radial MR images of 1-year- and 2-year-old bolts obtained by the proton density weighted SE sequence (Table 2). The solid line 'a' on the transverse MR images in Figure 2b indicates the plane of the radial section in Figure 2a. In transverse and longitudinal MR images, the area indicating highest intensity (whitish) was around the cambial zone probably including immature cambial derivatives in which all cells are living and contain cytoplasm (Fig. 2a; Cz). The boundary between phloem and the cambial zone could not be distinguished in the MR images. The major part of the xylem was indicated as of high intensity (Fig. 2a; CX). Individual tracheids which have a diameter of c. 20 μm (Fig. 1c; T) could, however, not be distinguished in the MR images. Images obtained by the T2 weighted sequence, that also detects water, indicated similar or higher contrast (Fig. 2b; Cz, CX).

In detailed observations, it was shown that MR signal intensities, that is, the brightness of the images, fluctuated between tissues that contain living cells such as cambial zone, cortex and pith, and also between current annual ring and inner rings in the sapwood (Fig. 2a). The cortex was darker than the cambial zone and conductive sapwood although cells are living in this tissue (Fig. 2b; Cor). The pith, which consists of

parenchymatous cells, showed also a low signal intensity in the MR images (Fig. 2; P). Latewood and compression wood indicated low signal intensity and were shown as dark bands in the cross section (Fig. 2; LW, CW). Inner annual rings showed a lower intensity than the current annual ring.

The surface image of three bolts cut from a healthy *Quercus serrata* branch (Fig. 1b) scanned at the same time was reconstructed from a FSPGR dataset (Fig. 3a). The sapwood of the specimen had been judged as normally conducting in optical observations of cut ends at harvest and by the results of our previous investigation (Kuroda & Yamada 1996). The diameter of large and small vessels of this species ranges from 200 to 300 μm and 20 to 30 μm, respectively (Fig. 1d; LV, SV). The cambial zone

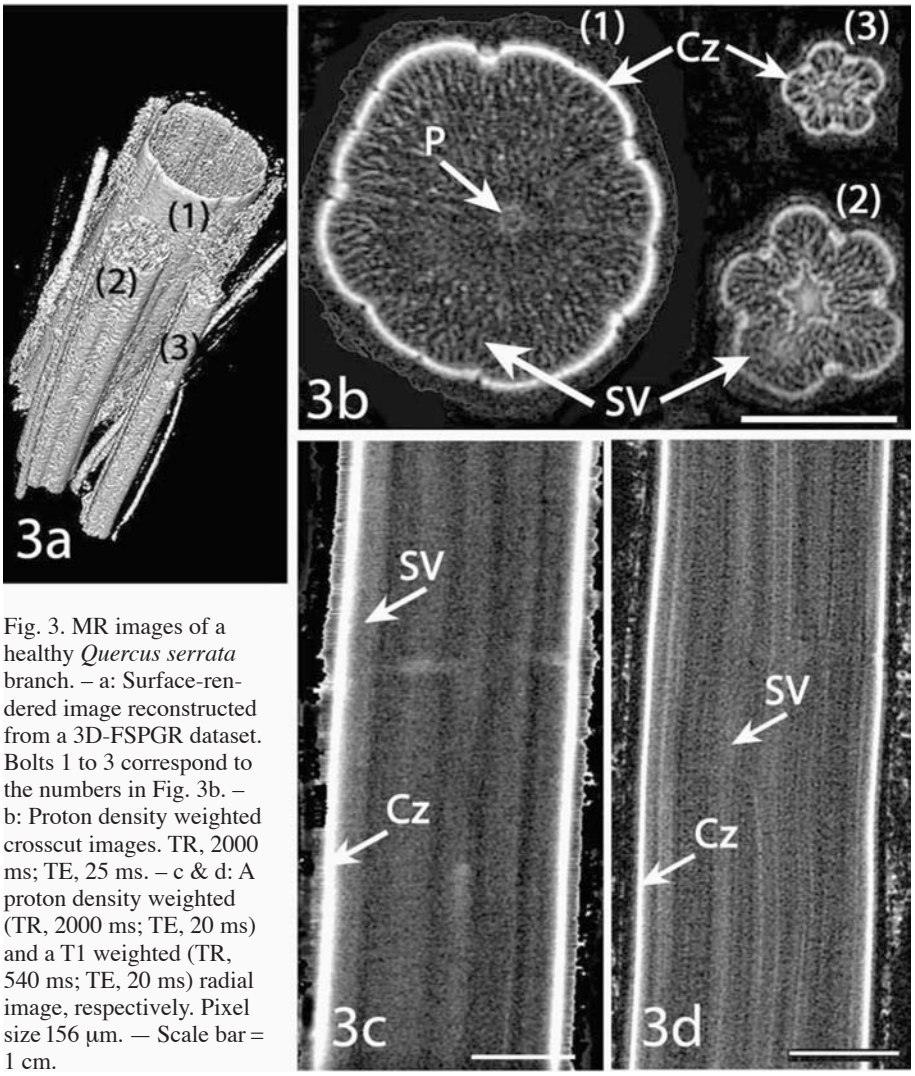

Fig. 3. MR images of a healthy *Quercus serrata* branch. – a: Surface-rendered image reconstructed from a 3D-FSPGR dataset. Bolts 1 to 3 correspond to the numbers in Fig. 3b. – b: Proton density weighted crosscut images. TR, 2000 ms; TE, 25 ms. – c & d: A proton density weighted (TR, 2000 ms; TE, 20 ms) and a T1 weighted (TR, 540 ms; TE, 20 ms) radial image, respectively. Pixel size 156 μm. — Scale bar = 1 cm.

showed the highest signal intensity in the MR images obtained by the proton density SE sequence in this hardwood species as well (Fig. 3b & c; Cz). In the cross-sectional MR images, the areas of high intensity in xylem were shown as wavy bright lines (Fig. 3b; SV), and coincided with the areas where the small vessels are arranged in a flame-like pattern (Fig. 1d; SV). Individual vessels narrower than 30 μm in diameter were, however, not distinguishable (Fig. 3b). Large vessels (Fig. 1b & d; LV) that are easily dehydrated by drought during summer or after harvest were not shown in the MR images (Fig. 3b). In the MR images obtained by SE sequences, the resolution of the images is equal to the pixel size. Pixel size = FOV / image size (512 μm). Therefore, the resolution of the images was theoretically 117 or 156 μm when the FOV was 60 or 80 mm, respectively (Table 2, Fig. 2 & 3). These values were larger than the diameter of small vessels. In addition, slice thickness less than 3 mm provided images with lower contrast, and the thicker slice around 5 mm lowered the resolution of the images. The areas occupied by the wood fibers (Fig. 1d; F) between vessels showed a very low intensity (Fig. 3b). Broad ray tissue and axial parenchyma were not detectable although they consist of living cells. The pith was not so dark as that of *Pinus densiflora*. In the radial image obtained by the proton density sequence, whitish zones that were extending longitudinally between darker zones were blurred (Fig. 3c; SV). The same radial image obtained by T1 weighted sequence showed clearer whitish areas in the xylem (Fig. 3d) corresponding to those in the proton density image, although the T1 weighted sequence is not aimed at the detection of water distribution.

Detection of dehydrated areas in trees infected with wilt diseases

In the stem of a pine seedling that had survived the infection with the pine wilt pathogen, a restricted area around the inoculated site was completely dehydrated and filled with air. The external appearance of the scanned area and inoculation wound was shown by surface rendering of a FSPGR dataset (Fig. 4a). The solid lines 'b' and 'c' in Figure 4a indicate the sites of cross sections in Figures 4b and 4c, respectively, and correspond to those in Figure 4d. In the crosscut MR images obtained by the proton density sequence, the air-filled xylem was pitch-black (Fig. 4b & c; DX), in contrast to the high intensity of the conducting xylem (Fig. 4b; CX). In the radial MR image, a similar dark area without MR signals extended about 3 cm longitudinally along the inoculation wound, and the boundary to the conducting area was very clear (Fig. 4d). A cambial zone that was not necrotic indicated a similar signal intensity as that in the MR images of healthy tree. The normal cortex, which consists of living parenchymatous cells, showed a medium intensity (Fig. 4b; Cor) which was lower than that in the cambial zone. Latewood adjacent to the cambial zone was as dark as that of a healthy pine tree (Fig. 2).

In the stem of oak saplings inoculated with *Raffaelea quercivora*, brownish discoloration that was formed as a reaction to the infection was detected by optical observation after the MR imaging (Fig. 5a, b & 6a; Dis). Discolored xylem that is called pathogenic heartwood or wound heartwood is known to be dehydrated and dysfunctional (Hillis 1987; Kuroda 2001; Kuroda & Yamada 1996). In the present specimens, the discolored xylem extended longitudinally above and below the inoculated site (Fig. 5a & b). The cambium and phloem were necrotic in the area just surrounding the inoculated sites

(Fig. 5a). In the crosscut MR images obtained by the proton density sequence, the discolored area in the xylem (Fig. 5a; Dis) did not show an MR signal and was completely black (Fig. 5c; Dis). Small vessels in a conducting area indicated the high-intensity MR signals (Fig. 5a–e; CX) in contrast to the lower intensity and vaguely whitish appearance of the partly discolored xylem (Fig. 5b, Dis; 5d). Dysfunctional large vessels were identified as black spots along annual ring boundaries (Fig. 5a & c; LV). Broad ray tissues were recognized as white radial streaks in this infected specimen (Fig. 5d; R). In the control specimen without fungal inoculation, the signal intensity was lower only in the narrow area just around the injury.

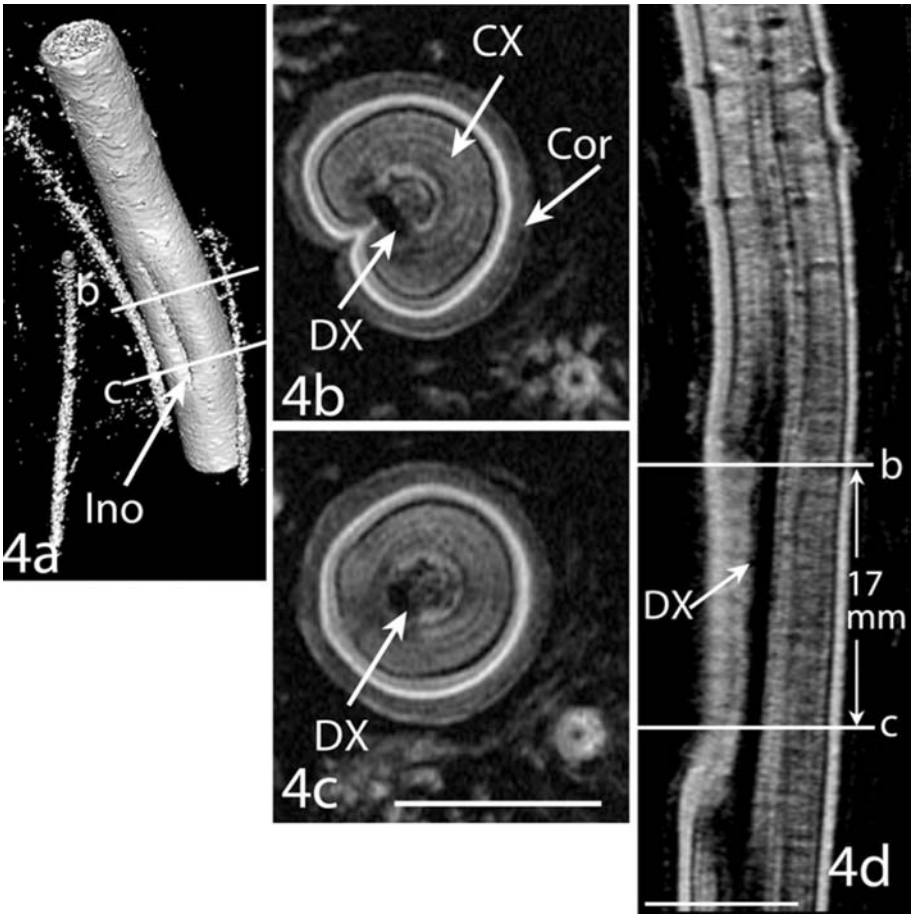

Fig. 4. Detection of a dehydrated area by MR imaging of a *Pinus densiflora* seedling that survived after inoculation with the wilt pathogen *Bursaphelenchus xylophilus*. – a: Surface-rendered images reconstructed from a FSPGR dataset. – b & c: Proton density crosscut images obtained from the section at solid lines b and c in Fig. 4d. Pixel size 156 μm. – d: Proton density radial image of the inoculated site. Pixel size 117 μm. Parameters of Fig. 4b–d: TR, 2000 ms; TE, 12 ms. — Scale bar = 1 cm.

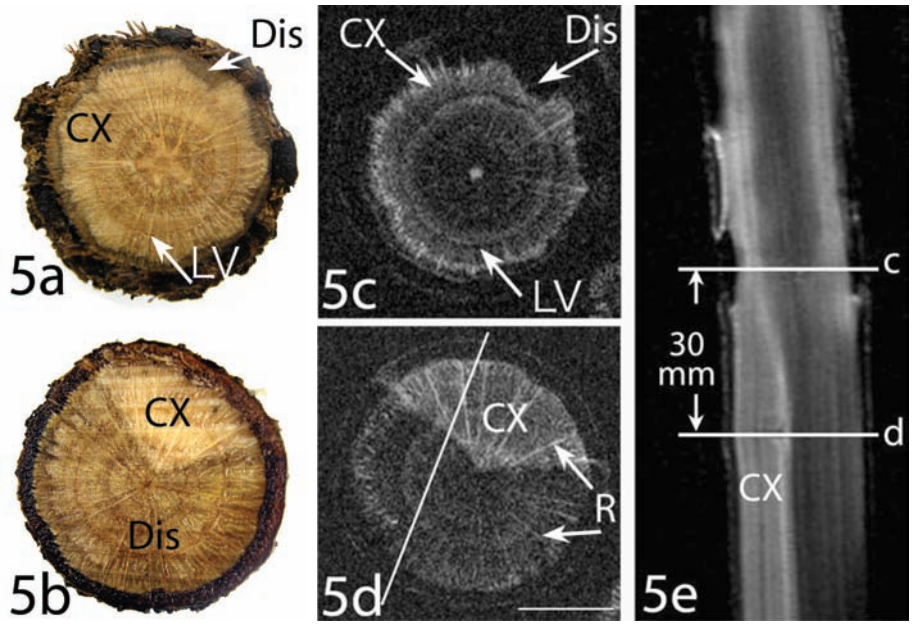

Fig. 5. *Quercus crispula* stem (Tree A) inoculated with the wilt pathogen *Raffaelea quercivora*. – a & b: Optical crosscut images. – c & d: Proton density MR images cut at the horizontal lines c and d in Fig. 5e and corresponding to optical images in 5a and 5b, respectively. TR, 2000 ms; TE, 22 ms. Pixel size 156 μm. – e: Longitudinal T1 weighted image cut at the solid line in Fig. 5d. TR, 1000 ms; TE, 22 ms. Pixel size 469 μm. — Scale bar = 1 cm.

T1 weighted imaging of infected tissue

T1 weighted sequences were obtained by both SE and FSPGR sequences (Table 2). T1 weighted images of *Quercus crispula* saplings inoculated with *Raffaelea quercivora* (Table 2) provided interesting results (Fig. 6). Figures 6a–c are crosscut optical images, water distribution obtained by proton density sequence, and the image obtained by T1 weighted sequence, respectively. These three figures show the same sections cut at the horizontal lines in Figure 6d & e. In the discolored xylem (Fig. 6a; Dis), fungal hyphae are present, and all cells were necrotic. In the T1 weighted images, the area of discolored xylem (Fig. 6a; Dis), which had shown low intensity in the proton density image due to the decrease of water (Fig. 6b; Dis), indicated a very high signal intensity (Fig. 6c & d; Dis). In the case of healthy materials, T1 weighted image (Fig. 3d) looked similar to the proton density image because the water-filled areas appeared whitish. The resolution of the T1 images obtained by the FSPGR sequence (Fig. 6c & d) was lower than that of the images obtained by the SE sequence (Fig. 6e). Therefore, the area of high intensity was shown as a slightly vague whitish mass in the image obtained by the FSPGR sequence. On the other hand, a three-dimensional analysis was possible from a FSPGR dataset that consisted of serial sections using the software ExsaVision Lite (Ziosoft Inc., Japan) and OsiriX Ver. 1.6 (Rosset *et al*. 2004). From images of various

cut-planes reconstructed from a FSPGR dataset, size of the affected area indicated by higher signal intensity was estimated. For example, the radial depth of the affected area was widest at the base of a twig in tree B (Fig. 6d; horizontal line) extending 15 mm from the cambium.

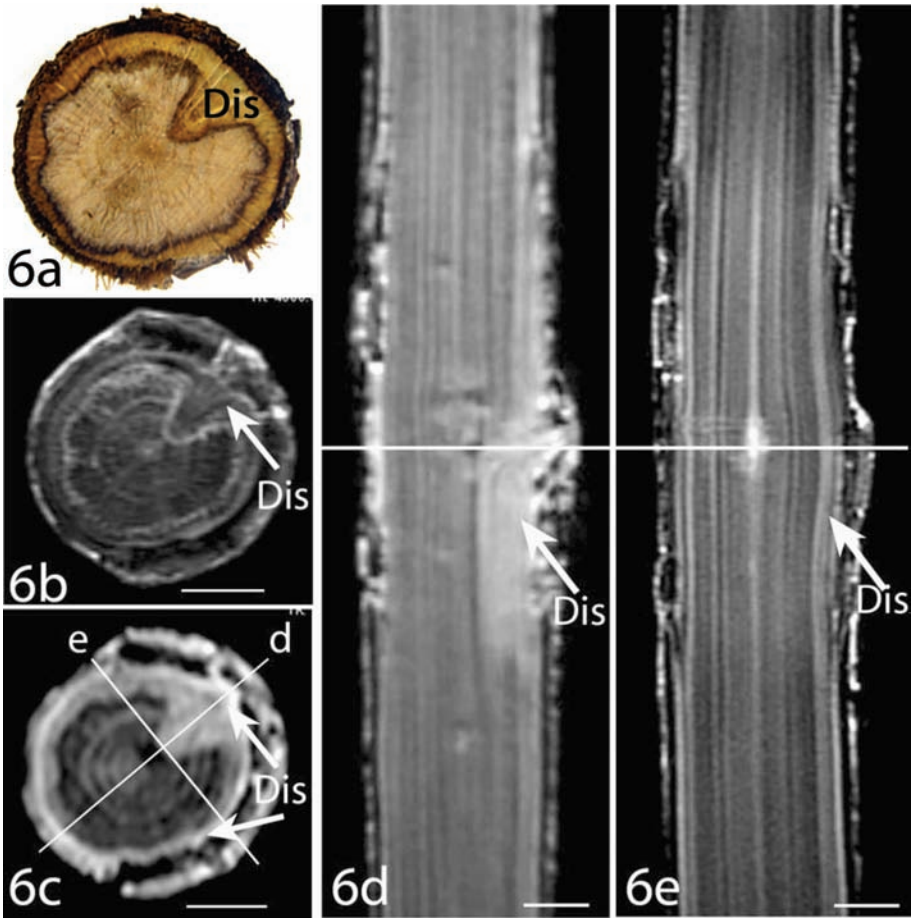

Fig. 6. Detection of the infected and necrotic area on the T1 weighted images of a *Quercus crispula* stem (Tree B) inoculated with *Raffaelea quercivora*. – a: Optical crosscut image. – b: Proton density image. TR, 4000 ms; TE, 21 ms. – c & d: T1 weighted cross and radial images obtained by the FSPGR sequence, respectively. TR, 8.3 ms; TE, 2.0 ms. Pixel size of 6b–d = 390 μm. – e: T1 weighted radial image obtained by the SE sequence. TR, 540 ms; TE, 20 ms. Pixel size 469 μm. – 6a–c show the same sections, cut at the solid lines in Fig. 6d & e. Images in Fig. 6d & e were cut at the solid lines d and e in Fig. 6c, respectively. — Scale bar = 1 cm.

DISCUSSION

The present experiments demonstrated that MR imaging by proton density SE sequences provide clear images of the water distribution in tree stems when TR is 2000 ms and TE is 12 to 25 ms, and also by T2 weighted sequences at TR is 4000 ms and TE is 80 ms. In addition to the pixel sizes, the slice thickness affected the quality of the images, because thinner slices weaken MR signals. The cross section sliced 3.0 to 4.0 mm thick provided the best images with higher contrast and sharpness for the SE sequences in the present experiment. In the images obtained by proton density and T2 weighted SE sequences, the xylem in which water-filled vessels and tracheids were abundant showed up as a whitish area in the MR images. The dehydrated area in the xylem that sometimes is formed by the infection with wilt pathogens is easily distinguished from the conductive area in these MR images. Completely dehydrated areas are pitch-black due to the lack of any MR signal. The conducting areas in the xylem of *Quercus* species was, however, not so bright as those of the *Pinus* species. This difference must be ascribed to the lower number of water conduits in hardwood than that in softwood. Radial proton-density MR images of the *Quercus serrata* stem, in which whitish longitudinal bands were observed between darker bands, also demonstrate that the area where small vessels filled with water are frequent is more whitish than the area where wood fibers are dominant.

Individual water conduits, tracheids and small vessels 20 to 30 μm in diameter, could not be identified although dysfunctional large vessels about 300 μm in diameter were identified as black spots on the cross section. Because the theoretical resolution of the images obtained from the SE sequence on the present imaging system was 117 μm in the highest case, individual tracheids and small vessels filled with water could not be distinguished, but their aggregations were visible. The higher quality of the MR images cited here compared to those in the former reports (Robinson *et al*. 2000; Pietrzak *et al*. 2002; Bucur 2003) must be due to the combination of parameters such as TR, TE and slice thickness, suitable for woody plants as well as the higher resolution that depends on the MR system used in the present experiments.

Local fluctuations of signal intensity were observed in the proton density MR images of healthy specimens. The lower intensity in latewood and compression wood than that in earlywood in pine stems, for instance, suggest dehydration in narrow tracheids that is known to occur during summer draught (Sperry & Tyree 1988), or may be a reflection of the small quantity of water surrounded by thick tracheid walls. The weaker MR signals obtained from the inner annual rings of a *Pinus densiflora* tree in this experiment and of a *Eucalyptus nitens* tree (Barry *et al*. 2001) than those from current annual rings suggest lower water conductivity and partial dehydration in the inner rings. The negative MR signals from the large vessels of a *Quercus serrata* branch harvested in September is consistent with the hypothesis of the easy dehydration and dysfunction of large vessels during summer draught (Zimmermann 1983). The precise value of moisture content in small volumes of xylem is actually difficult to measure, as reported by Barry *et al*. (2001), who emphasized that MR images detect slight changes of moisture content that cannot be measured by gravimetric methods. This MR imaging technique will be useful to investigate daily or seasonal dehydration of water conduits as reported

by Holbrook *et al*. (2001) when a proper MR sequence fit for the purpose is selected. Physiological information of xylem dysfunction in relation to heartwood formation can also be obtained. The conducting water conduits, however, cannot be distinguished from those conduits just accumulating sap by the MR sequences used in this experiment. To analyse the conductivity of conduits, additional techniques are necessary as reported by Ilvonen *et al*. (2001).

There were significant differences in the MR signal intensity between various living tissues in the tree stems. The signal intensity of tree tissues that contain living cells should be interpreted in distinction from those of water conduits that contain only water. Extremely high intensity in the cambial zone, exceeding that in water-filled tracheids suggests the contribution of some other substances that might be related to high metabolic activity in cambial cells. The relatively darker images of cortex, phloem, and pith suggest that an MR signal becomes strong only when a certain volume of cavity is completely filled with water as in the case of water conduits. In addition, the MR signal intensity from living tissues may vary in relation to the percentage of living cells included in the tissue and may vary also depending on the metabolic activity of constituent cells.

T1 weighted SE sequence obtained by the combination of TR, 540 ms, and TE, 20 ms, as an example, and FSPGR sequence obtained by the TR, 8.3 ms and TE, 2 ms provided a bright image of the area affected by fungal infection. The area of highest intensity roughly coincided with the area of fungal distribution, necrotic lesion, and pathogenic heartwood. T1 weighted images were obviously different from the proton density images in the case of specimens infected with pathogen. In medical studies, T1 weighted images are used to find areas rich in fat and protein (NessAiver 1996) and are used to detect lesions. Some substances that are produced in plant tissues as a reaction to fungal activity might resemble fat or protein. At present, we do not know whether the T1 weighted images of the plant material can be used in the same way as in medical research, because substances that provide strong MR signals have not been specified yet in the plants. Still, T1 weighted images will be useful to find anomalies associated with infections. On the other hand, T1 weighted images have often been used for the analysis of water distribution in healthy plants (Robinson *et al*. 2000; Wagner *et al*. 2000). Also in the present investigation, T1 weighted sequence sometimes provided similar and much clearer images of the healthy tree stems than the proton density sequence as shown in Figure 3d. The MR images obtained by the T1 weighted sequences can, however, not be used for an analysis of water distribution in plants.

MR imaging of softwood and hardwood stems enables the observation of: 1) dehydrated and dysfunctional areas in proton density and T2 weighted images, and 2) areas affected by infection, such as necrotic lesion and pathogenic heartwood in T1 weighted images. Further technical improvement will be necessary to study the properties of anomalies in the infected tissue by T1 weighted sequences in detail. Three-dimensional MR images of infected trunks that were reconstructed from the data of the FSPGR sequence are helpful to recognize the volume of the infected area. Although *in vivo* experiments with this technique are applicable to only juvenile trees at present, periodical imaging of living trees will provide useful data on their physiology and pathology. Based on the present results, investigations on the wilting mechanism of trees infected with diseases have been started.

ACKNOWLEDGEMENTS

We acknowledge Ziosoft, Inc., Japan for free use of their software ExsaVision Lite, and Dr. Utsuzawa of MRTechnology, Inc., Tsukuba, Japan, for his kind advice on the parameters that should be considered in the technical discussion on MR imaging. We also wish to thank Dr. Y. Takahata, Kansai Research Center, Forestry & Forest Products Research Institute for his kind permission to use oak specimens inoculated with the pathogen.

REFERENCES

Barry, K., R. Pearce, S. Evans, L. Hall & C. Mohammed. 2001. Initial defense responses in sapwood of *Eucalyptus nitens* (Maiden) following wounding and fungal inoculation. Physiol. & Molec. Plant Pathol. 58: 63–72.

Bucur, V. 2003. Nondestructive characterization and imaging of wood. Springer-Verlag, Berlin, Heidelberg.

Elster, A.D. 1994. Questions and answers in magnetic resonance imaging. Mosby-Year Book, St. Louis.

Fromm, J.H., I. Sautter, D. Matthies, J. Kremer, P. Schumacher & C. Ganter. 2001. Xylem water content and wood density in spruce and oak trees detected by high-resolution computed tomography. Plant Physiol. 127: 416–425.

Glidewell, S.M., B. Williamson, G.H. Duncan, J.A. Chudek & G. Hunter. 1999. The development of blackcurrant fruit from flower to maturity: a comparative study by 3D nuclear magnetic resonance (NMR) micro-imaging and conventional histology. New Phytol. 141: 85–98.

Hillis, W.E. 1987. Heartwood and tree exudates. Springer-Verlag, Berlin, Heidelberg, New York.

Holbrook, N.M., E.T. Ahrens, M.J. Burns & M.A. Zwieniecki. 2001. In vivo observation of cavitation and embolism repair using magnetic resonance imaging. Plant Physiol. 126: 27–31.

Ilvonen, K., L. Palva, M. Peramaki, R. Joensuu & R. Sepponen. 2001. MRI-based D2O/H2O-contrast method to study water flow and distribution in heterogeneous systems: Demonstration in wood xylem. J. Magnetic Resonance 149: 36–44.

Kozlowski, T.T. & S.G. Pallardy. 1997. Physiology of woody plants. Ed. 2. Academic Press, San Diego.

Kuroda, K. 1991. Mechanism of cavitation development in the pine wilt disease. Eur. J. For. Path. 21: 82–89.

Kuroda, K. 2001. Responses of Quercus sapwood to infection with the pathogenic fungus of a new wilt disease vectored by the ambrosia beetle *Platypus quercivorus*. J. Wood Sci. 47: 425–429.

Kuroda, K. 2002. The mechanism of tracheid cavitation in trees infected with wilt diseases: 17–23. Proc. IUFRO Working party 7.02.02 Shoot and foliage diseases, Meeting at Hyytiala, Finland, 17–22 June 2001.

Kuroda, K. 2003. Recent degradation of conifer plantations in the Kansai district of Japan. Bull. Forestry and Forest Products Res. Inst. 2: 247–254.

Kuroda, K. & T. Yamada. 1996. Discoloration of sapwood and blockage of xylem sap ascent in the trunks of wilting Quercus spp. following attack by *Platypus quercivorus*. J. Jap. For. Soc. 73: 84–88 [In Japanese with English summary].

Kuroda, K., T. Yamada, K. Mineo & H. Tamura. 1988. Effects of cavitation on the development of pine wilt disease caused by *Bursaphelenchus xylophilus*. Ann. Phytopath. Soc. Japan 54: 605–615.

Manion, P.D. & D.H. Griffin. 1992. Resistance in aspen to Hypoxylon canker. In: Blanchette & Biggs (eds.), Defense mechanisms of woody plants against fungi: 308–320. Springer-Verlag, Berlin, Heidelberg.

NessAiver, M. 1996. All you really need to know about MRI Physics. Simply Physics, Baltimore.

Pearce, R., B. Fisher, T. Carpanter & L. Hall. 1997. Water distribution in fungal lesions in the wood of sycamore, *Acer pseudoplatanus*, determined gravimetrically and using nuclear magnetic resonance imaging. New Phytol. 135: 675–688.

Pietrzak, L.N., J. Fregeau-Reid, B. Chatson & B. Blackwell. 2002. Observations on water distribution in soybean seed during hydration processes using nuclear magnetic resonance imaging. Canad. J. Plant Sci. 82: 513–519.

Robinson, A., C.J. Clark & J. Clemens. 2000. Using H-1 magnetic resonance imaging and complementary analytical techniques to characterize developmental changes in the *Zantedeschia* Spreng. tuber. J. Experim. Bot. 51: 2009–2020.

Rosset, A., L. Pysher, L. Spadola & O. Ratib. 2004. OsiriX, http://homepage.mac.com/rosset antoine/osirix/, UCLA, Los Angeles, California.

Sakamoto, Y., Y. Yamada, Y. Sano, Y. Tamaki & R. Funada. 2004. Pathological anatomy of Nectoria canker on *Fraxinus mandshurica* var. *japonica*. IAWA J. 25: 165–174.

Schneider, H., N. Wistuba, R. Reich, H.-J. Wagner, W.L.H. & U. Zimmermann. 2000. Minimal- and noninvasive characterization of the flow-fore pattern of higher plants. In: M. Terazawa (ed.), Tree sap II: 77–91. Hokkaido University Press, Sapporo.

Sperry, J. & M.T. Tyree. 1988. Mechanism of water stress-induced xylem embolism. Plant Physiol. 88: 581–587.

Tyree, M.T. & J.S. Sperry. 1989. Characterization and propagation of acoustic emission signals in woody plants: Towards an improved acoustic emission counter. Plant, Cell and Environ. 12: 371–382.

Wagner, H.J., H. Schneider, S. Mimiets, N. Wistuba, M. Rokitta, G. Krohne, A. Hasse & U. Zimmermann. 2000. Xylem conduits of a resurrection plant contain a unique lipid lining and refill following a distinct pattern after desiccation. New Phytol. 148: 239–255.

Yamaguchi, T., Y. Maruyama & Y. Sakamoto. 2003. Evaluation of forest health and viability suitable for sustainable forest management in Hokkaido, northern Japan: Three years trial and perspective for the future: 13–18. Proc. C&I Symp. in Tsukuba, 23–26 Oct. 2002.

Zimmermann, M.H. 1983. Xylem structure and the ascent of sap. Springer-Verlag, Heidelberg, Berlin, New York.